Research Article

The extracellular matrix of dystrophic mouse diaphragm accounts for the majority of its passive stiffness and is resistant to collagenase digestion

Ross P. Wohlgemuth [a], **Ryan M. Feitzinger** [a], **Kyle E. Henricson** [a,b], **Daryl T. Dinh** [a], **Sarah E. Brashear** [a] and **Lucas R. Smith** [a,c*]

a - ***Department of Neurobiology,*** *Physiology, and Behavior, University of California Davis, USA*
b - ***Department of Chemistry and Biochemistry,*** *University of California Santa Cruz, USA*
c - ***Department of Physical Medicine and Rehabilitation,*** *University of California Davis, USA*

Correspondence to Lucas R. Smith:*One Shields Avenue, 196 Briggs Hall NPB Davis, CA 95616-5270.
lucsmith@ucdavis.edu (L.R. Smith)
https://doi.org/10.1016/j.mbplus.2023.100131

Abstract

The healthy skeletal muscle extracellular matrix (ECM) has several functions including providing structural integrity to myofibers, enabling lateral force transmission, and contributing to overall passive mechanical properties. In diseases such as Duchenne Muscular dystrophy, there is accumulation of ECM materials, primarily collagen, which results in fibrosis. Previous studies have shown that fibrotic muscle is often stiffer than healthy muscle, in part due to the increased number and altered architecture of collagen fibers within the ECM. This would imply that the fibrotic matrix is stiffer than the healthy matrix. However, while previous studies have attempted to quantify the extracellular contribution to passive stiffness in muscle, the outcomes are dependent on the type of method used. Thus, the goals of this study were to compare the stiffness of healthy and fibrotic muscle ECM and to demonstrate the efficacy of two methods for quantifying extracellular-based stiffness in muscle, namely decellularization and collagenase digestion. These methods have been demonstrated to remove the muscle fibers or ablate collagen fiber integrity, respectively, while maintaining the contents of the extracellular matrix. Using these methods in conjunction with mechanical testing on wildtype and D2.*mdx* mice, we found that a majority of passive stiffness in the diaphragm is dependent on the ECM, and the D2.*mdx* diaphragm ECM is resistant to digestion by bacterial collagenase. We propose that this resistance is due to the increased collagen cross-links and collagen packing density in the ECM of the D2.*mdx* diaphragm. Taken altogether, while we did not find increased stiffness of the fibrotic ECM, we did observe that the D2.*mdx* diaphragm conveyed resistance against collagenase digestion. These findings demonstrate how different methods for measuring ECM-based stiffness each have their own limitations and can produce different results.

Introduction

The skeletal muscle extracellular matrix (ECM) consists of connective tissue that surrounds the entire muscle organ as well as individual fascicles and myofibers [1]. The ECM helps with many functions within muscle including maintaining structural integrity of muscle fibers, providing a fibrous scaffold for regeneration, transmitting force from myofibers to tendons, and contributing to overall passive mechanical properties. Thus, having an intact ECM is highly important to active and passive muscle function as well as regeneration and muscle growth. However, in muscle diseases such as Duchenne Muscular Dystrophy (DMD) there are pathological changes to the muscle that lead to accumulation of ECM components and severe deficits in matrix function (fibrosis) [2–5]. In DMD this stems from a

mutation to dystrophin which renders it non-functional and leaves the muscle fibers highly susceptible to contraction-induced damage [6–8]. Over time the muscle encounters progressive damage that results in chronic cycles of incomplete regeneration [3,9,10]. During the attempted repair of muscle fibers, resident fibro-adipogenic progenitors secrete new matrix components to provide scaffolding for new muscle tissue [11,12]. However, since the regeneration is incomplete the secreted matrix remains and builds up, resulting in impaired muscle function and fibrosis.

There are many components of the skeletal muscle ECM that are upregulated in fibrosis. Among them are proteoglycans such as biglycan and decorin, which can regulate collagen fibrillogenesis and alter TGFβ activity [13–15]. Fibronectin, a soluble protein, is also highly upregulated in DMD and is important to satellite cell function, an essential part of muscle regeneration [13,16]. Along with fibronectin, fibrin can help form fibrous networks during wound healing that provides structure to the ECM [13,17,18]. However, the primary component of the muscle matrix is fibrillar collagen, which is the dominant load bearer of the ECM [1,19]. While collagen content increases significantly in fibrotic muscle, it also displays architectural shifts that alter its mechanical properties [20–23]. In several models of fibrotic muscle diseases, collagen cross-links, biochemical linkages between collagen molecules, are upregulated compared to muscle from healthy controls [20,24,25]. These collagen cross-links have been associated with increased muscle passive stiffness, an increase in passive tension for a given increase in muscle length, and also make the collagen fibers more difficult to digest by matrix metalloproteinases [20,23,26–29]. Other architectural changes such as collagen fiber density, area, and alignment are also increased in models of fibrosis, particularly in the D2.*mdx* mouse, a model for DMD [4,20,21,23]. The D2.*mdx* mouse presents more severe phenotype than the C57.*mdx* mouse, particularly in the areas of muscle strength and collagen content, which are especially reduced and upregulated in the D2.*mdx* mouse, respectively. This is due in part to a mutation to annexin A6 and increased TGFβ signaling in the D2.*mdx* mouse which reduces the muscle's ability to repair sites of damaged sarcolemma and increases transcription of fibrogenic genes, respectively [30,31]. Many parameters of collagen architecture are associated with increased stiffness in D2.*mdx* muscles and are known to regulate the mechanical properties of other tissues, e.g. collagen fiber alignment in tendon is associated with increased tensile stress [32,33]. Previous studies have independently demonstrated that the ECM accounts for a large fraction of muscle stiffness and that fibrotic muscles are generally stiffer than healthy controls [20,34–39]. However, the majority of these studies only utilize a single method to calculate extracellular-based stiffness and do not directly compare healthy and fibrotic muscles. Importantly, the efficacy between methods for quantifying extracellular stiffness in muscle has not been extensively looked at and is important for ensuring that the results of different studies can be corroborated effectively. Thus, the main goal of this study was to use two independent methods to assess the extracellular stiffness from healthy and fibrotic skeletal muscle. We decided to compare a method that would give a measure of overall ECM mechanical properties as well as one that would relate specifically to the collagen matrix, as it plays a large role in ECM passive mechanics.

Based on previous studies, we selected decellularization and collagenase digestion as the methods for quantifying the mechanical properties of the overall ECM and collagen matrix, respectively. The decellularization treatment, which has been described previously, was designed to lyse and remove the muscle fibers without damaging the ECM to allow the measurement of overall ECM-based mechanical properties [37,40]. The collagenase digestion treatment, which was adapted from previous methods [41], was designed to cleave collagen molecules and ablate the mechanical properties of the collagen matrix. Thus, our study was designed to measure the mechanical properties of untreated muscle, decellularized muscle ECM, and intact collagen matrices. We hypothesized that the ECM and collagen matrix would account for the majority of passive stiffness in fibrotic muscle, and that fibrotic muscle would have greater ECM-based and collagen matrix-based passive stiffness than wildtype muscle. We found a majority of passive stiffness was maintained in the decellularized diaphragms of both genotypes and the D2.*mdx* diaphragm exhibited resistance to collagenase digestion.

Results

Characterization and validation of decellularization and collagenase treatments

We assessed the effects of decellularization (decell) and collagenase (coll-ase) digestion on healthy and fibrotic muscle in order to expand on previous characterizations of these methods. There were no differences in body weight, muscle length, or physiological cross-sectional area (PCSA) between wildtype (WT) and D2.*mdx* mice and muscles (Fig. 1A–C Fig. S1A-B).We found that diaphragm (DP) and extensor digitorum longus (EDL) decellularized matrices (DCM) experienced a significant drop in muscle mass compared to untreated muscle, while the soleus (SOL) did not exhibit a significant effect of treatment (Fig. 1D, Fig. S1C). Collagenase digested (CD) muscles had significantly decreased weight for diaphragm, soleus, and EDL muscles (Fig. 1E, Fig. S1D).

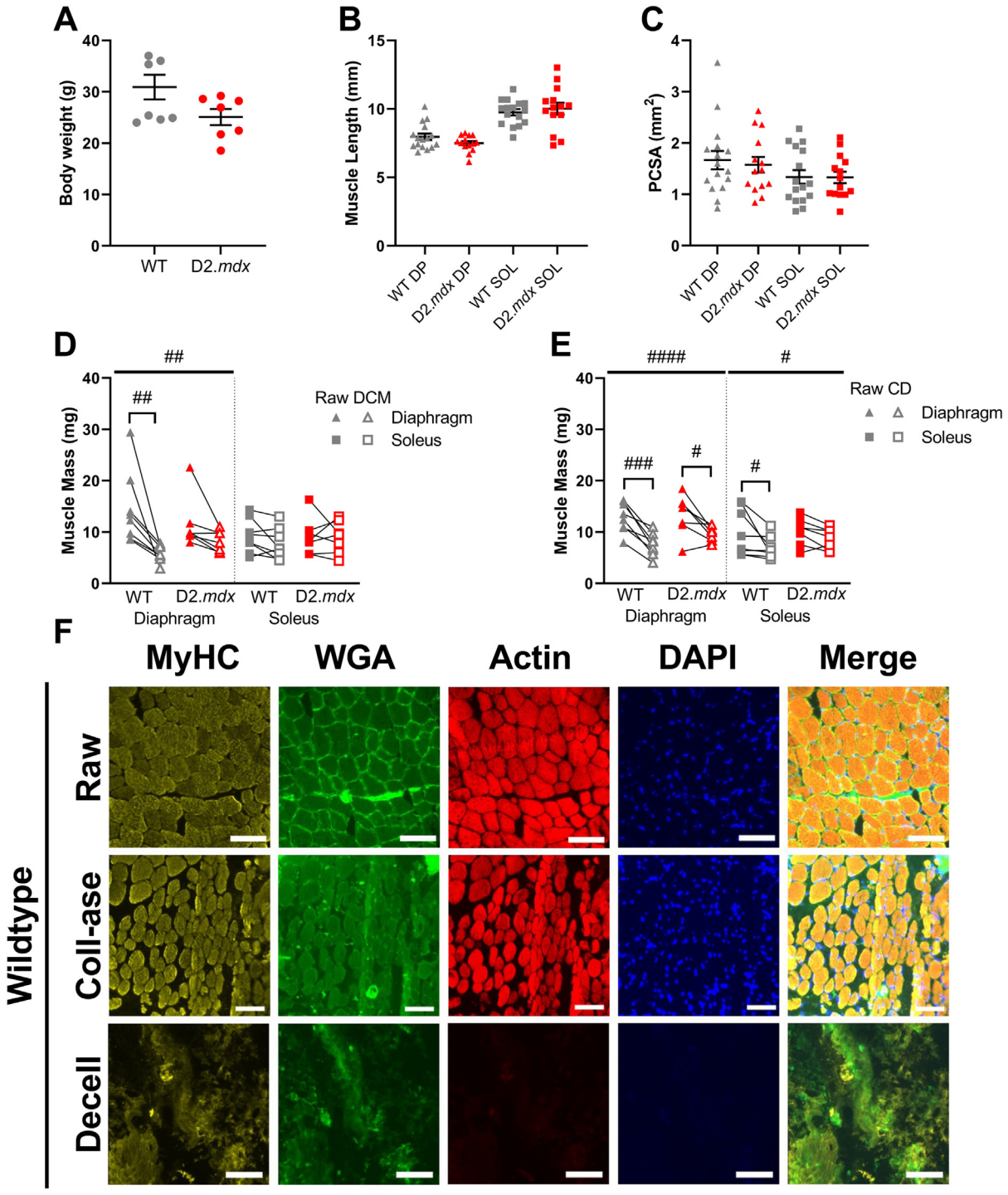

Fig. 1. Muscle characteristics with respect to treatment. (A) There was no significant difference in bodyweight between wildtype and D2.*mdx* mice. (B) Optimum muscle length (L_o) was not significantly different between wildtype and D2.*mdx* muscles. (C) Muscle PCSA was not significantly different between wildtype and D2.*mdx* muscles. (D) Decellularization treatment reduced the sample weight of diaphragm muscles but not solei. (E) Collagenase digestion treatment reduced the sample weight of diaphragm and soleus muscles. (F) Representative fluorescent images of raw, collagenase (coll-ase), and decellularized (decell) wildtype muscles. Scale bars are equal to 100 μm. Flat bars represent two-way ANOVA significant main effects by treatment: $^{\#}p < 0.05$, $^{\#\#}p < 0.01$, $^{\#\#\#\#}p < 0.0001$. Bracketed bars represent post-hoc Sidak test significant differences by treatment: $^{\#}p < 0.05$, $^{\#\#}p < 0.01$, $^{\#\#\#}p < 0.001$. DP = diaphragm, SOL = soleus, DCM = decellularized matrix, CD = collagenase digested, MyHC = myosin heavy chain, WGA = wheat germ agglutinin, Coll-ase = collagenase, Decell = decellularized.

Fluorescent imaging showed that myosin heavy chain (MyHC) and actin were prominent in the untreated (raw) tibialis anterior (TA) muscles as well as the collagenase digested muscles in both the wildtype and D2.*mdx* mice (Fig. 1F, Fig. S2). However, decellularization treatment severely reduced the actin present in the sample while myosin heavy chain signal was partially lost and disrupted. Similarly, nuclear integrity seemed to be preserved in the raw and collagenase muscles while it was largely absent after decellularization. Lastly, there appeared to be a reorganization of ECM in the collagenase digested and decellularized samples compared to the raw tissues. The collagenase samples appeared to have less ECM surrounding the fibers while the decellularized muscles had a major loss of this structural motif, likely due to the absence of muscle fibers. These observations of the decellularized muscles are in line with the use of this method in a previous study which showed the maintenance of some myosin protein, a large drop in actin abundance, and a dramatic drop in tissue DNA content [37]. Overall, we did not observe differences by genotype between the fluorescent images of wildtype and D2.*mdx* tibialis anterior muscles following either treatment.

While the decellularization protocol has been previously validated in conjunction with muscle mechanical testing and ECM properties, the collagenase digestion treatment has not been validated in the same fashion. Thus, we wanted to demonstrate the effectiveness of collagenase in ablating the integrity of the collagen matrix as well as affecting mechanical properties of the muscle. To this end we ran experiments on three wildtype female mice to assess the mechanical properties of diaphragm and soleus muscles before and after a 1-hour collagenase treatment or a 1-hour sham treatment which consisted of the same protocol without the collagenase enzymes. We found that muscle mass was reduced following collagenase treatment in both the diaphragm and soleus muscles (Fig. S3A). Additionally, we observed a stark reduction in the proportion of elastic stiffness in the collagenase digested muscles compared to the sham and raw muscles of the diaphragm and soleus (Fig. S3B). To assess the amount of collagen left over in the matrix as well as the degree of cross-linking following either treatment, we ran hydroxyproline and collagen solubility assays on the muscles tested. We found that there were no differences in total collagen content or percent insoluble (cross-linked) collagen between treatments in either muscle (Fig. S3C–D). Thus, these experiments showed that collagenase treatment was successful in ablating the integrity of the collagen matrix as evidenced by the dramatic drop in elastic stiffness without a change in collagen content.

To follow up the experiments validating the effectiveness of collagenase in ablating collagen integrity, we sought to assess whether a longer exposure to collagenase would further degrade the collagen matrix and reduce mechanical stiffness. Thus, we used a cohort of three D2.*mdx* female mice to test whether a 2-hour treatment of collagenase would have more severe effects than a 1-hour treatment. We found again that muscle mass was reduced following either treatment in the diaphragm, but not in the soleus (Fig. S4A). As expected, we observed significant declines in the proportion of elastic stiffness maintained after 1-hour and 2-hour collagenase treated muscles; however, we did not find a significant difference between the 1-hour and 2-hour groups (Fig. S4B). Further, we did not observe significant differences in collagen content or cross-linking between the untreated, 1-hour, and 2-hour groups (Fig. S4C–D). Thus, it was evident that a 2-hour exposure to collagenase did not substantially reduce the integrity of the collagen matrix or the mechanical stiffness of the diaphragm and soleus muscles relative to the 1-hour treatment.

Muscle mechanical properties following decellularization and collagenase treatments

To compare the mechanical properties between wildtype and D2.*mdx* skeletal muscle and its native ECM, we measured the passive stress and stiffness of diaphragm, EDL, and soleus muscles before and after a decellularization treatment. In the diaphragm and soleus there were significant declines in passive stiffness due to the decellularization treatment, but there was no difference with treatment in the EDL (Fig. 2A, Fig. S1E). We also observed a significant increase in elastic stiffness of D2.*mdx* soleus muscles compared to wildtype, but no genotype differences in the diaphragm or EDL. Interestingly we found that the decellularized diaphragm was less elastic than the raw diaphragm muscles, but this effect was not present in the soleus or EDL muscles (Fig. 2B, Fig. S1G). Further, the D2.*mdx* diaphragm demonstrated a lower degree of elasticity than the wildtype, which is in line with previous reports [21,23,42,43]. In order to quantify the contribution of the decellularized ECM to passive stress, we compared the percent of elastic stress that was maintained in the decellularized matrices to that of the original, raw muscle. This analysis showed no significant differences in any of the muscles tested related to genotype or strain (Fig. 2C–D, Fig. S1I). Taken altogether, we found that while decellularization reduced the elastic stiffness by approximately 25–60% in diaphragm and soleus muscles, there were only genotype differences in the stiffness between wildtype and D2.*mdx* soleus ECMs.

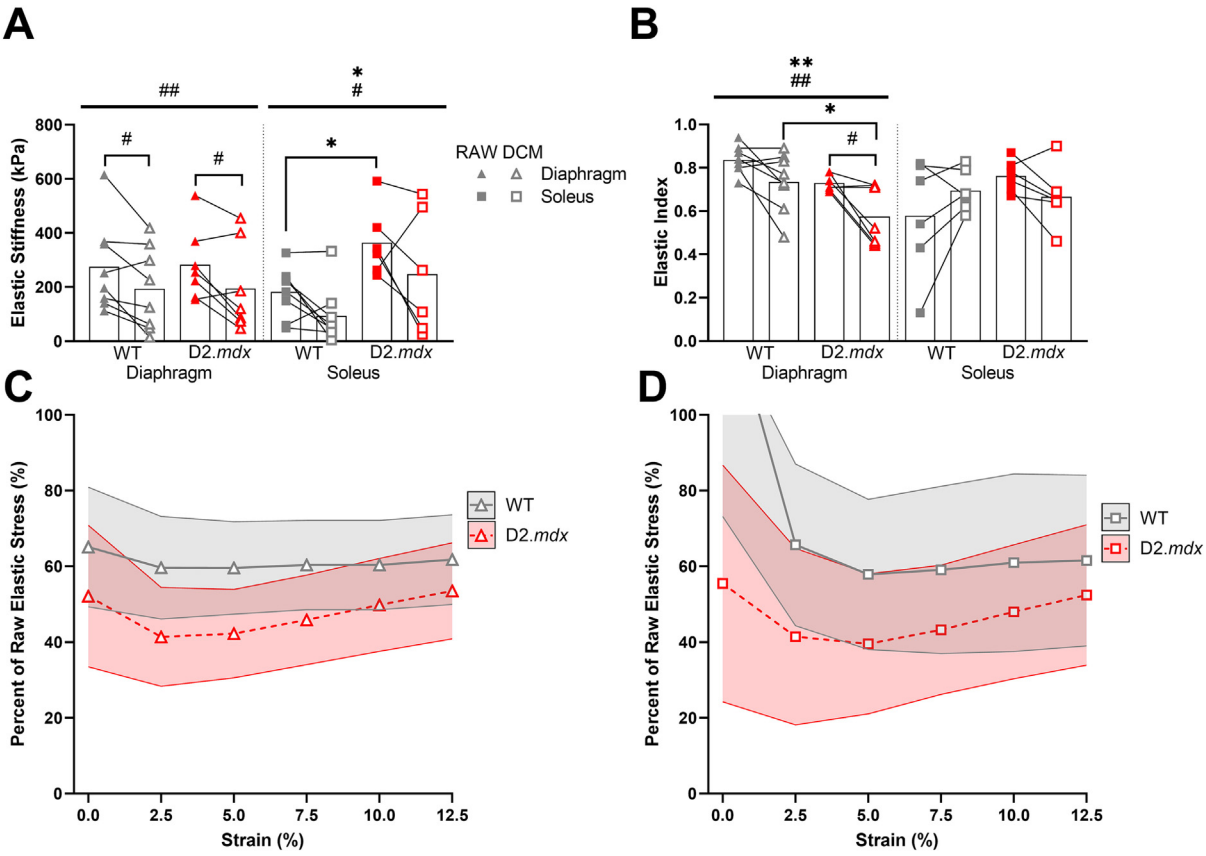

Fig. 2. Decellularization reduced muscle passive stiffness and elasticity. (A) Decellularization treatment reduced elastic stiffness in diaphragm and soleus muscles. D2.*mdx* solei were stiffer than wildtype. (B) Decellularization treatment reduced the elastic index (elasticity) of the diaphragm muscles, but not soleus. D2.*mdx* diaphragms were less elastic than wildtype. (C) About half of passive stress was maintained in wildtype and D2.*mdx* diaphragm muscles following decellularization, but there was no difference in passive stress between genotypes. (D) There was no difference in passive stress of decellularized soleus muscles between genotypes. Shaded areas represent ± SEM. Flat bars represent two-way ANOVA significant main effects by treatment: $^{\#}p < 0.05$, $^{\#\#}p < 0.01$, $^{\#\#\#}p < 0.001$; and by genotype: $^{*}p < 0.05$, $^{**}p < 0.01$. Bracketed bars represent post-hoc Sidak test significant differences by treatment: $^{\#}p < 0.05$, $^{\#\#}p < 0.01$.

Next, we compared the mechanical properties between wildtype and D2.*mdx* skeletal muscle with and without the integrity of the collagen matrix by measuring passive stress and stiffness in diaphragm, EDL, and soleus muscles before and after a 1-hour treatment with collagenase. Collagenase treatment was effective in significantly reducing the stiffness of all muscles tested as well as lowering their elasticity (Fig. 3A–B, Fig. S1F,H). There was also an effect of genotype on diaphragm elastic stiffness such that the D2.*mdx* diaphragm was stiffer than the wildtype. Although this effect was not seen in the decellularization experiments, it has been observed previously [23,42,43]. Although there was not a significant interaction effect between genotype and treatment in the diaphragm, there was a trend showing the D2.*mdx* diaphragm maintained a higher degree of stiffness following collagenase than the wildtype diaphragm. In line with this observation, the proportion of elastic stress that remained after collagenase digestion trended higher in the D2.*mdx* diaphragm compared to wildtype (Fig. 3C). Further, there was a significant effect of interaction between genotype and strain in the elastic stress of the diaphragm. This result was not seen in the elastic stress of the soleus, but there was a significant effect of strain such that more elastic stress was preserved at higher strains in the soleus following collagenase (Fig. 3D). No significant effects on elastic stress were present in the D2.*mdx* EDL (Fig. S1J). Therefore, these data convey that collagenase was effective in reducing the elastic stiffness in all muscles tested, but the D2.*mdx* diaphragm showed a higher proportion of elastic stress preserved at higher strains compared to wildtype.

Collagen matrix characteristics following collagenase treatment

Following mechanical analysis of the muscles before and after each treatment, we quantified

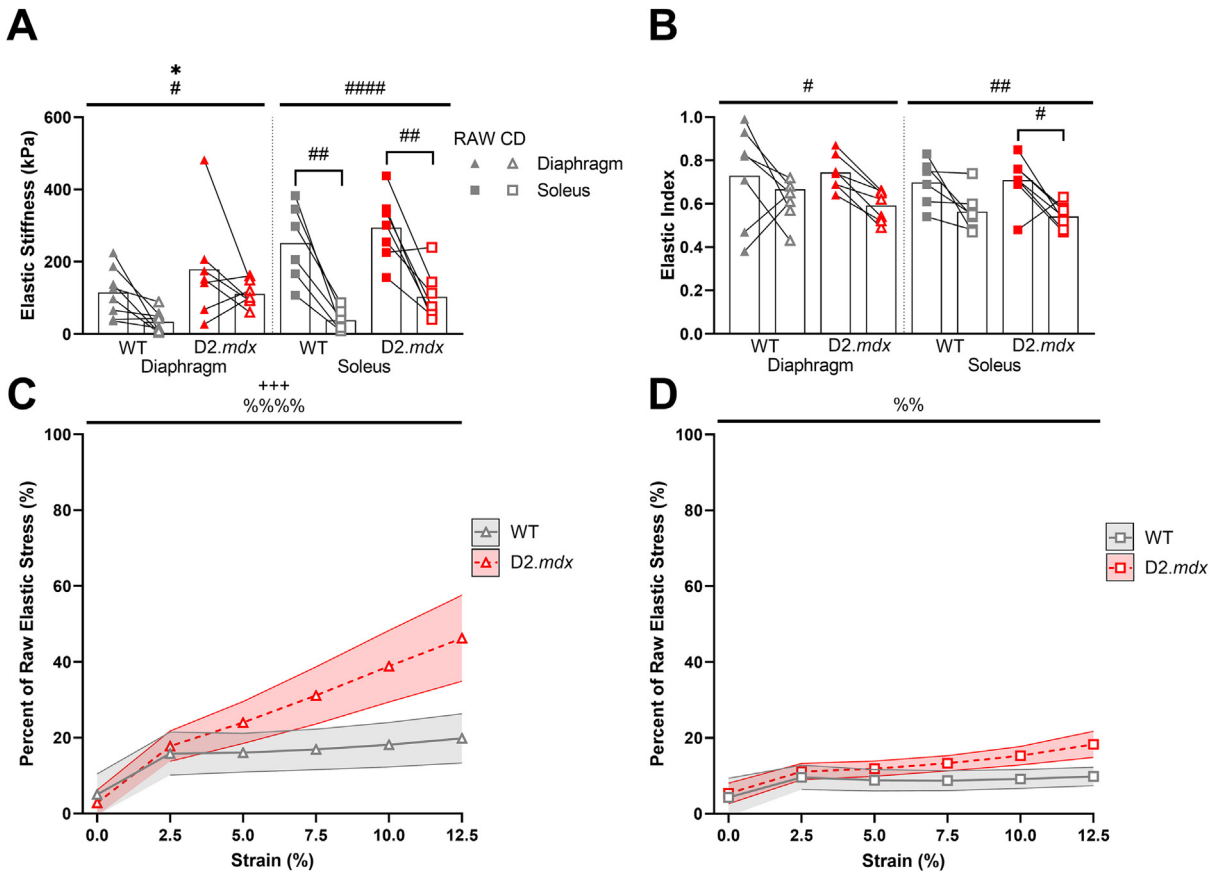

Fig. 3. Collagenase reduced muscle passive stiffness and elasticity, but dystrophic diaphragm exhibited resistance to digestion. (A) Collagenase treatment reduced elastic stiffness in diaphragm and soleus muscles. The D2.*mdx* diaphragm showed greater elastic stiffness than wildtype. (B) Collagenase treatment reduced elasticity of diaphragm and soleus muscles. (C) Collagenase digested dystrophic diaphragm muscles maintained a higher proportion of elastic stress at higher strains than wildtype muscles. (D) Soleus muscles maintained a higher proportion of elastic stress at higher strains following collagenase digestion. Shaded areas represent ± SEM. Flat bars represent two-way ANOVA significant main effects by treatment: $^{\#}p < 0.05$, $^{\#\#}p < 0.01$, $^{\#\#\#}p < 0.001$; by genotype: $^{*}p < 0.05$, by strain: $^{\%\%}p < 0.01$, $^{\%\%\%\%}p < 0.0001$, and by strain and genotype: $^{+++}p < 0.001$. Bracketed bars represent post-hoc Sidak test significant differences by treatment: $^{\#}p < 0.05$, $^{\#\#}p < 0.01$.

collagen content and cross-linking using the hydroxyproline and collagen solubility assay to assess if the collagen matrix was still present within the muscle sample after treatment. We found that there was no effect of decellularization or collagenase digestion on total collagen content in any muscle (Fig. 4A, Fig. S1K). Nevertheless, the D2.*mdx* diaphragm showed significantly higher collagen content than the wildtype. Similarly, collagen cross-links, which have been shown to make the ECM stiffer and harder to degrade, were also higher in the D2.*mdx* diaphragm compared to the wildtype [20,23,26–29] (Fig. 4B). There was a significant effect of collagenase on collagen cross-linking in the soleus such that the collagenase treatment appeared to reduce the proportion of collagen cross-links. This effect was present in the EDL to a lesser degree, but not in the diaphragm (Fig. S1L, Fig. 4B). From these data we conclude that neither decellularization or collagenase digestion reduced total collagen content in the muscle. We also note that the increased collagen cross-links in the D2.*mdx* diaphragm, which can make the collagen matrix harder to degrade, may be related to the maintained elastic stiffness and stress in the D2.*mdx* diaphragm following collagenase treatment compared to the wildtype.

To further investigate how the D2.*mdx* diaphragm could maintain passive mechanical properties following collagenase treatment, we used Picrosirius red staining and imaging to assess the collagen area around muscle fibers and the packing density of collagen fibers within each muscle before and after treatment with collagenase (Fig. 4C). We found that the D2.*mdx* diaphragm had a higher percent of area occupied by ECM and a higher proportion of densely packed collagen compared to the wildtype (Fig. 4D–E). Even though there were no differences by genotype or treatment for ECM

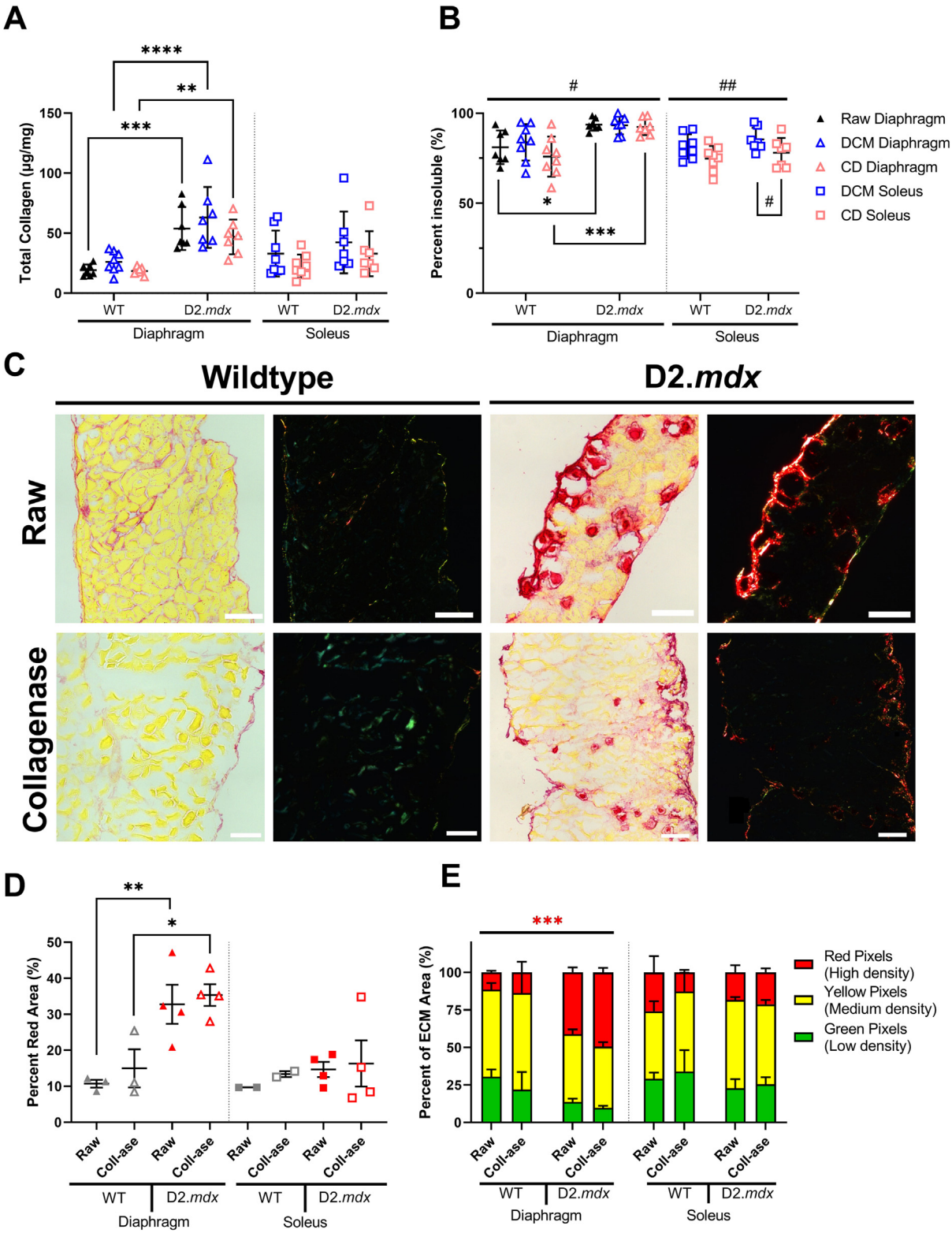
A
Total Collagen (µg/mg)
150
100
50
0
****
**
***
WT
D2.mdx
WT
D2.mdx
Diaphragm
Soleus
B
Percent insoluble (%)
100
50
0
#
##
*
***
#
WT
D2.mdx
WT
D2.mdx
Diaphragm
Soleus
Raw Diaphragm
DCM Diaphragm
CD Diaphragm
DCM Soleus
CD Soleus
C
Wildtype
D2.mdx
Raw
Collagenase
D
Percent Red Area (%)
50
40
30
20
10
0
**
*
Raw
Coll-ase
Raw
Coll-ase
Raw
Coll-ase
Raw
Coll-ase
WT
D2.mdx
WT
D2.mdx
Diaphragm
Soleus
E
Percent of ECM Area (%)
100
75
50
25
0
***
Raw
Coll-ase
Raw
Coll-ase
Raw
Coll-ase
Raw
Coll-ase
WT
D2.mdx
WT
D2.mdx
Diaphragm
Soleus
Red Pixels
(High density)
Yellow Pixels
(Medium density)
Green Pixels
(Low density)

area in the EDL and soleus, we saw a decrease in loosely packed collagen in the D2.*mdx* EDL compared to wildtype (Fig. 4D–E, Fig. S1M–N). Since densely packed collagen may sterically interfere with the action of collagenase on cleavage sites, the dense collagen matrix in the D2.*mdx* diaphragm could provide resistance to collagenase that is not present to the same degree in the soleus and EDL muscles.

Discussion

In this study we compared the passive mechanical contributions of the ECM and collagen fibers in wildtype and dystrophic skeletal muscle. Using two methods, decellularization and collagenase digestion, we were able to compare how different methods that quantify extracellular-based passive mechanics can produce different results. Nevertheless, our study demonstrated that the skeletal muscle ECM is a major component of muscle stiffness and that the integrity of the collagen matrix, with respect to collagenase, is related to its architecture. Overall, we found that the decellularized matrix accounts for approximately 65% of muscle passive stiffness and up to 60% of passive stress (Fig. 5A–C). The absence of muscle cells also led to a loss in elasticity in the decellularized matrices. The collagenase digestion affected muscles in a more variable manner, reducing overall stiffness by up to 85% and stress by up to 90% in all muscles except the D2.*mdx* diaphragm (Fig. 5A–C). The D2.*mdx* diaphragm showed it maintained more elastic stress after decellularization than the wildtype diaphragm and the D2.*mdx* soleus. Thus, the D2.*mdx* diaphragm showed greater resistance to collagenase digestion than its wildtype counterpart and another dystrophic muscle. These collagenase digested samples also exhibited declines in elasticity. These results emphasize the differences between two methods of quantifying extracellular-based muscle mechanics and imply that collagen architecture can affect the results from these experiments.

While we hypothesized that the fibrotic decellularized ECM from the D2.*mdx* mice would have greater stiffness than the wildtype decellularized ECM, we observed that even in the diaphragm, which exhibits severe fibrosis in the D2.*mdx* mouse, there was no significant difference in elastic stiffness between genotypes. Our second hypothesis was that the fibrotic collagen matrix would have a greater contribution to stiffness than the wildtype collagen matrix. Although we were successful in reducing passive stiffness with collagenase digestion, we found that the fibrotic diaphragm collagen matrix was resistant to collagenase digestion. Thus, it is difficult to conclude exactly how much stiffness the collagen matrix accounts for in each genotype based on the collagenase experiments. Taken together, we demonstrated the efficacy of two methods for quantifying extracellular-based stiffness in skeletal muscle and showed that the majority of stiffness in D2.*mdx* diaphragm is dependent on the ECM, which is also resistant to digestion by collagenase.

Using decellularization and collagenase to measure extracellular-based passive mechanics

One of the goals of this study was to compare two methods of measuring extracellular-based stiffness. In our study we showed that while decellularization and collagenase each have merit in measuring mechanical and biochemical properties of the muscle ECM, they are not always easily comparable. For one, while decellularization is a method that preserves the whole ECM, the collagenase method targets collagens specifically. Thus, the corresponding measurements of the collagenase digested samples will say more about the specific role of collagen to mechanical properties instead of the overall ECM. Even though collagen fibers are the

Fig. 4. Collagen matrix characteristics following decellularization and collagenase. (A) Total collagen was higher in D2.*mdx* diaphragm muscles compared to wildtype. There were no significant effects of treatment on total collagen. (B) Percentage of insoluble collagen, a measure of cross-linked collagen, was significantly higher in D2.*mdx* diaphragms compared to wildtype. There was a decrease in the percent of insoluble collagen in the collagenase treated D2.*mdx* soleus compared to the decellularized soleus. (C) Representative brightfield and polarized light images of Sirius red stained diaphragm sections. (D) The D2.*mdx* diaphragm had a significantly higher percentage of muscle occupied by ECM than the wildtype. (E) The D2.*mdx* diaphragm had a significantly higher proportion of densely packed collagen than the wildtype, but there was no effect of collagenase on collagen packing density. Scale bars are equal to 100 μm. Flat bars represent two-way ANOVA significant main effects by treatment: $^{\#}p < 0.05$, $^{\#\#}p < 0.01$; and by genotype: $^{***}p < 0.001$. Bracketed bars represent post-hoc Sidak test significant differences by treatment: $^{\#}p < 0.05$; and by genotype: $^{*}p < 0.05$, $^{**}p < 0.01$, $^{***}p < 0.001$, $^{****}p < 0.0001$. (For interpretation of the references to colour in this figure legend, the reader is referred to the web version of this article.)

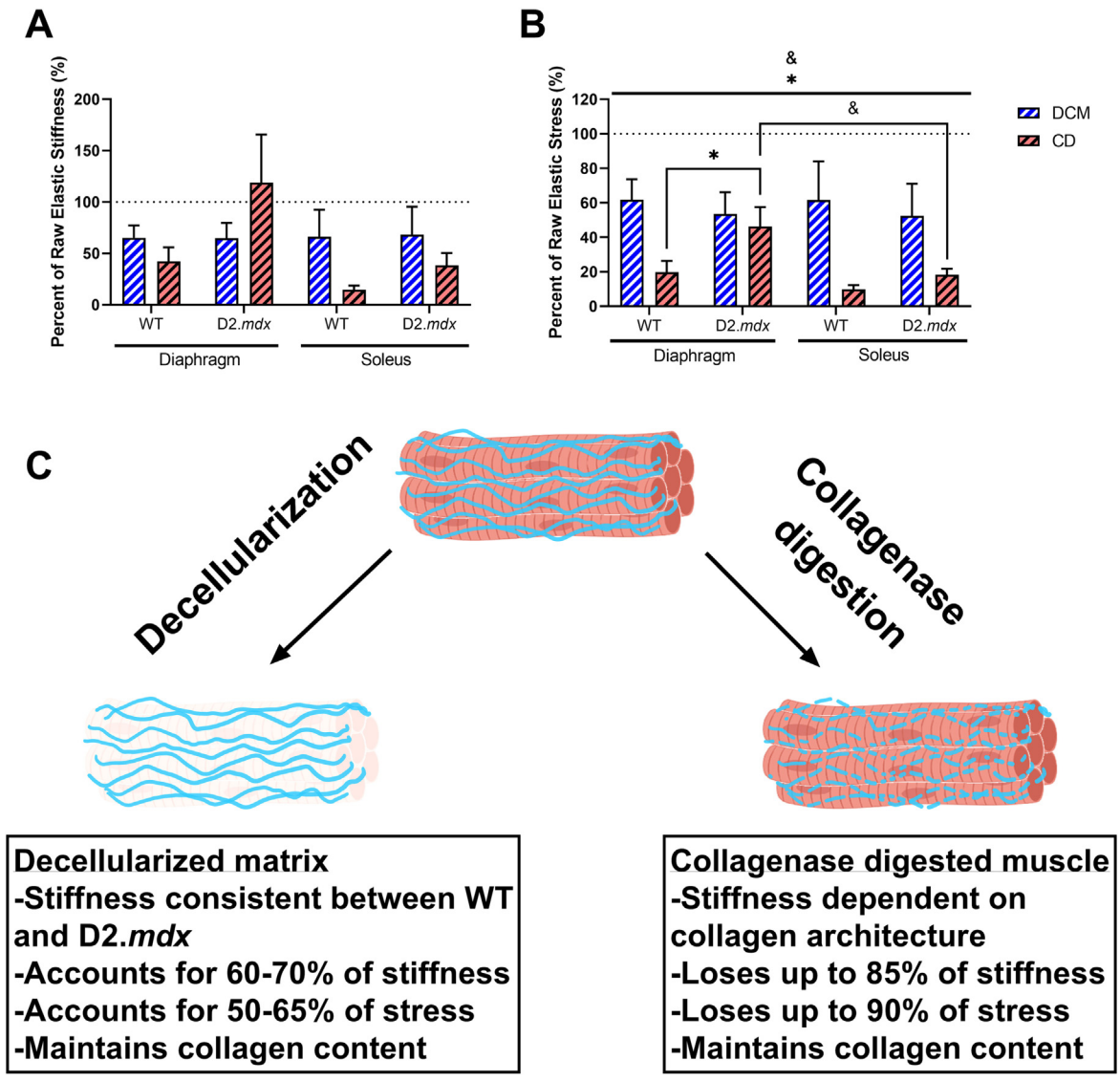

Fig. 5. Summary of mechanical properties of decellularized matrices and collagenase digested muscles. (A) A majority of elastic stiffness is maintained in the decellularized diaphragm and soleus. The collagenase digested D2.*mdx* diaphragm maintains a higher proportion of stiffness than the wildtype. This effect is present in the D2.*mdx* soleus to a lesser degree. (B) Similar to (A), a majority of elastic stress at 12.5% strain is maintained in the decellularized diaphragm and soleus. The collagenase digested D2.*mdx* diaphragm maintains a significantly greater proportion of stress than the wildtype. This effect is present in the D2.*mdx* soleus to a lesser degree. (C) Schematic of the effects of decellularization and collagenase treatments on skeletal muscle mechanics and collagen content. Flat bars represent two-way ANOVA significant main effects by muscle: $^{\&}p < 0.05$; and by genotype: $^{*}p < 0.05$. Bracketed bars represent post-hoc Sidak test significant differences by muscle: $^{\&}p < 0.05$; and by genotype: $^{*}p < 0.05$. Panel C of this figure was created using BioRender.com.

primary load-bearers of the muscle ECM, there are other nuanced aspects of the muscle ECM including the architecture of collagen fibers (e.g. collagen cross-links, fiber alignment, and number of perimysial collagen cables) as well as other matrix components that could impact stiffness in a way that cannot be measured using collagenase digestion [19,20,22,23]. Nevertheless, collagenase digestion could serve as a useful method for relating the collagen architecture of the muscle ECM to its resistance to digestion or turnover. Many aspects of the collagen matrix may improve its resistance to collagenase digestion including collagen cross-linking, collagen fiber packing density, and tension in collagen fibers [21,27–29,44,45]. In fibrosis, the collagen matrix often shows an imbalance in collagen turnover through its progressive accumulation of collagen, potentially due to a resistance to colla-

gen degradation. Using the collagenase digestion treatment could provide a measure for the resistance of a collagen matrix to degradation by MMPs as well as the potential reduction in muscle stiffness that could be achieved by matrix remodeling factors. While collagenase is useful in this sense, the resistance to digestion exhibited by the D2.*mdx* diaphragm makes the method less useful in quantifying the mechanical properties of the muscle collagen matrix. This can be visualized in Fig. 5 by adding the proportion of elastic stiffness maintained in the D2.*mdx* diaphragm after decellularization and collagenase. Clearly, the combined stiffness would be much greater than 100% of the original stiffness, showing that these methods are not calculating opposite contributions to muscle mechanical properties. Overall, it seems that when trying to quantify the overall stiffness of the ECM, decellularization may be a superior method, especially when working with muscles that may be resistant to collagenase or other forms of matrix digestion. For an approach that relates the integrity of the collagen matrix to enzymatic degradation, using collagenase may be better suited than decellularization.

Differences in healthy and fibrotic ECM mechanical properties or lack thereof

Based on previous studies which show that passive stiffness is increased in fibrotic skeletal muscle, we expected the fibrotic ECM to demonstrate increased mechanical properties compared to wildtype ECM [20,23,39,42,43]. Instead we found no differences between wildtype and D2.*mdx* decellularized ECM stiffness in any muscle tested. This may have been due to the small sample size used in our study compared to others, although we attempted to combat this by performing repeated mechanical testing before and after treatment to increase statistical power. Another possibility is that the cellular components of the muscle, namely the myofibers, account for the difference in stiffness between wildtype and D2.*mdx* muscles. However, previous studies do not support the hypothesis that dystrophic/fibrotic muscle fibers are stiffer than wildtype fibers [39,46,47]. One explanation could be related to how the decellularized ECM architecture is affected by the treatment. It is possible that the removal of myofibers causes the ECM layers to deform in the absence of cellular structure. Further, previous studies have shown that the slack length of the decellularized ECM is reduced and the tissue appears to swell following the treatment [40]. Previous reports from our lab and others have emphasized the importance of ECM architecture to mechanical properties, so these alterations in gross tissue structure may have significant impacts on our measurements of the decellularized matrix mechanics [20,22,23].

We also expected the collagen matrix to have greater stiffness in the dystrophic muscle than the wildtype. In order to test this we applied a collagenase solution to the muscle to ablate the integrity of the collagen fibers and reduce their mechanical properties. Although we intentionally used the maximum recommended concentration of collagenase to fully ablate the integrity of the collagen matrix, it is evident that collagenase was not totally effective in ablating collagen fiber integrity and stiffness in the D2.*mdx* diaphragm, likely due to the high proportion of collagen cross-links and high collagen density. Considering the time course experiment between a 1-hour and 2-hour collagenase treatment, it also appeared that a longer treatment with collagenase did not further reduce the stiffness of the D2.*mdx* diaphragm. This would suggest that it is not the increased amounts of collagen content that are preventing the total digestion of the collagen matrix, but the architecture of the matrix itself. The D2.*mdx* soleus and EDL, which have been shown in previous studies to have increased collagen cross-links, exhibited less resistance to the collagenase treatment compared to the diaphragm [20,23]. Thus, our collagenase experiments, while useful in providing a measure for collagenase resistance, were unable to show a change in stiffness between the collagen matrices in wildtype and dystrophic muscles. Future attempts to quantify the stiffness of the collagen matrix in skeletal muscle should account for the impact of matrix architecture on the effectiveness of collagenase.

Collagenase resistance in fibrosis and potential therapeutics

In this study we showed that in the D2.*mdx* diaphragm there is a high proportion of collagen cross-links and densely packed collagen which could make the collagen matrix more difficult to digest by bacterial collagenase. This provides evidence that the structure of the ECM within the D2.*mdx* diaphragm makes it less susceptible to collagen turnover and more conducive to accumulation of collagen. A similar shift from loose to densely packed collagen was observed in the D2.*mdx* EDL, although the degree of collagen cross-linking was not upregulated in the D2.*mdx* EDL compared to wildtype. We also did not observe a significant change in the elastic stiffness of collagenase-digested D2.*mdx* EDL compared to wildtype. Thus, it may be the case that a combination of both high proportions of densely packed and cross-linked collagen fibers may be necessary for matrix resistance to collagenase digestion. Given that the D2.*mdx* diaphragm has altered collagen architecture at early adulthood, it seems possible that the native matrix architecture within the diaphragm perpetuates a positive feedback loop such that increased collagen cross-links and collagen fiber density make the collagen matrix more difficult to turnover, causing more accumulation and further

increases in cross-links and fiber number. Previous studies have tested various inhibitors of collagen cross-links in order to prevent or reverse fibrosis, to different amounts of success [23,48–50]. Given the remarkable level of resistance the D2.*mdx* diaphragm exhibits against bacterial collagenase, it is evident that the inhibition of collagen cross-links could serve as a useful therapeutic in combating muscle fibrosis. Additionally, bacterial collagenases similar to the one used in this study have been shown to break up connective tissue and reduce stiffness in patients with Dupuytren's contracture or Peyronie's disease [51–55]. In combination, inhibiting collagen cross-linking and applying collagenase could serve as a two-factor therapy for extensive remodeling and turnover of fibrotic scar tissue in muscle contractures [56]. However, each of these potential therapeutics come with their own limitations in terms of effectiveness and side effects [55,57,58]; additionally, the diaphragm is largely inaccessible for injections. For muscles that are accessible to injections, such as those in the upper and lower limbs, the use of collagen cross-link inhibitors and collagenases may provide a great benefit for increasing ECM turnover and promoting muscle growth.

Limitations

This study was successful in comparing two methods of measuring the extracellular contributions to stiffness in healthy and dystrophic skeletal muscle. However, we acknowledge that there are multiple limitations to our study. With respect to the decellularization treatment, while it is clear that the components of the matrix are still present in the sample following decellularization, it is unknown whether swelling or shortening of the slack length has an effect on the sample's collagen architecture. Swelling of the decellularized matrix would cause the collagen fibers to expand outward and become less aligned with the long axis [40,59]. Considering previous studies have demonstrated a link between collagen fiber alignment and mechanical stiffness, these changes in matrix organization during decellularization could impact the resultant mechanical properties [20,22,23]. Future studies could perform further analysis on decellularized matrices to see if their architecture is altered compared to the original muscle sample.

Our collagenase digestion protocol was based off of a previous study [41]. In trial runs we found that 2 h of collagenase exposure to wildtype limb muscles rendered them unable to withstand the mechanical testing protocol. We also saw a lack of a drop in mass with 2-hour collagenase treatment that was unexpected given the small, but significant loss with 1-hour collagenase. This may have been due to the differences between experiments with only D2.*mdx* mice being used for the 2-hour collagenase test. Additionally, we acknowledge that there may be some effect of collagenase on the cellular integrity of myofibers based on our Sirius red images. Since it is clear that the primary subcellular structures such as actin and myosin in addition to the ECM components are still present in the collagenase digested samples, we believe that the collagenase treatment still provides an accurate measure of the contribution of the intact collagen matrix to muscle mechanical properties. As stated previously, specific aspects of collagen architecture can reduce the effectiveness of collagenase. In the D2.*mdx* diaphragm, which has high amounts of collagen cross-links and densely packed collagen fibers, the collagenase treatment was less adept in reducing muscle mechanical properties. Although this clouds the true mechanical contribution of the collagen matrix within the dystrophic diaphragm, it provides evidence for the impact that altered collagen architecture can have on the ECM's susceptibility to turnover. Finally, we acknowledge that there are differences based on sex and age in the D2.*mdx* mouse related to bodyweight and some measures of strength, among others [60]. However our experiments were not designed to test sex-based differences and we do not report them in this study.

Conclusions and next steps

Overall, we found that there was no difference in decellularized ECM stiffness by genotype, but the ECM accounted for the majority of stiffness in the diaphragm muscles. Also, in the D2.*mdx* diaphragm there was a clear resistance to collagenase activity that was paralleled with high proportions of collagen cross-links and collagen fiber density within the matrix. Taken together, this study shows that the skeletal muscle ECM is a mechanically important tissue and in fibrosis there can be collagen architectural changes that affect the susceptibility of the matrix to digestion by collagenase. These findings would be well supplemented by future studies analyzing the impact of further aspects of collagen architecture on collagen fiber susceptibility to collagenase as well as the effects of combined cross-linking inhibitor and collagenase treatment on the prevention and reduction of muscle fibrosis.

Experimental procedures

Ethical approval

All experiments involving animals were approved by the University of California, Davis Institutional Animal Care and Use Committee under IACUC protocol #22579.

Animal handling

DBA/2J (wildtype) and D2.B10-Dmd*mdx*/J (D2.*mdx*) mice were maintained in the UC Davis

Teaching and Research Animal Care Services (TRACS) facility. They were housed on a 12:12 light–dark cycle and given *ad libitum* access to water and food. Mice used in the primary cohort (wildtype male N = 7, wildtype female N = 1; D2.*mdx* male N = 6, D2.*mdx* female N = 1) were between 20 and 25 weeks of age when sacrificed. Female mice used in validation experiments (wildtype N = 3, D2.*mdx* N = 3) were between 30 and 35 weeks. Mice used in Sirius red analyses (wildtype female N = 3, D2.*mdx* male N = 4) were 27–41 weeks of age.

Muscle isolation

Mice were anesthetized with 2.5% Isoflurane gas in 1 L/min oxygen. Soleus, extensor digitorum longus (EDL), tibialis anterior (TA), and gastrocnemius muscles were collected from the lower limbs while the mice were under anesthesia. Following collection of the hindlimb muscles, euthanasia by cervical dislocation was done while mice were under anesthesia. Diaphragm muscles were then collected following cervical dislocation. Soleus, EDL, and diaphragm muscles were used for mechanical testing while TA and gastrocnemius muscles were used for histological and biochemical analyses, respectively. Soleus, EDL, and diaphragm muscles were stored in oxygenated Ringer's solution (Sodium Chloride, Potassium Chloride, Calcium Chloride dihydrate, Potassium Phosphate Monobasic, Magnesium Sulfate, 4-(2-Hydroxyethyl)piperazine-1-ethanesul fonic acid (HEPES), Glucose) after collection and during mechanical testing. TA and gastrocnemius muscles were either exposed to decellularization, collagenase digestion, or neither treatment prior to freezing and storage. TA muscles were pinned on cork and embedded in OCT for flash freezing in liquid nitrogen cooled isopentane. Gastrocnemius muscles were flash frozen in liquid nitrogen. Soleus, EDL, and diaphragm muscles were mechanically tested, treated with decellularization or collagenase, and then mechanically tested again before being flash frozen in liquid nitrogen. All muscles were stored at −80 °C. These muscle isolation methods are similar to previous studies [20,23].

Passive muscle mechanics

After isolation of the soleus and EDL, 7–0 sutures were cinched at the myotendinous junctions. A strip of diaphragm muscle cut along the myofiber angle was tied with 7–0 suture at the central tendon and the ribs. Suture loops were attached to the 300C-LR-Dual-Mode motor arm and force transducer (Aurora Scientific) in a bath of 28 °C oxygenated Ringer's solution similar to previous reports [20,23,61,62]. The optimum length for isometric force contraction (L_o) was estimated using a series of twitches as the muscle was incrementally stretched using the 701C stimulator (Aurora Scientific). The length at which the strongest twitch occurred was set as the L_o length. This length was measured using calipers between the sutures at either myotendinous junction. The muscle length (L_m), mass (m), ratio of fiber length to L_o (L_f/L_o), and density ($\rho = 1.06$ g/cm^3) were used to calculate the physiological cross-sectional area (PCSA; $PCSA = m/(L_o \bullet (L_f/L_o) \bullet \rho)$ [63]. In cases where the L_o could not be determined from the series of twitches, the L_o length was estimated using the result of the matched contralateral muscle.

Starting at L_o raw muscles underwent a passive mechanical protocol that consisted of preconditioning and held stretch steps. The preconditioning steps occurred before each held stretch step and were characterized by lengthening the muscle 2.5% beyond L_o at a rate of 1 Hz for 5 s. The held stretch steps were characterized by stretching the muscle 2.5% beyond L_o at a rate of 1 L_o/s and held at this length for 120 s. Preconditioning and held stretch steps were continued up to 5, 7.5, 10, and 12.5% strains using increments of 2.5% of L_o. The stiffness was reported as the slope of the quadratic fit to the plot of stress (tensile force per PCSA) and strain values. Elastic stiffness was the slope of this fit with stress values recorded at the end of the 120 s held stretch step while dynamic stiffness was the slope of the fit with the maximum stress values over the held stretch steps. Elastic index or elasticity was defined as the ratio between elastic and dynamic stiffness. Muscles that failed before 10% were not considered in the analysis of mechanical data. This technique is similar to other studies [21,64,65]. Following either collagenase digestion or decellularization, muscle samples were mechanically tested and analyzed in the same manner as the raw muscles.

Decellularization protocol

Tissue decellularization was performed based on a previous study [37]. Following muscle isolation and/or mechanical testing EDL, soleus, and diaphragm muscles were pinned at L_o on cork. Gastrocnemius muscles were each cut in half longitudinally prior to decellularization and were pinned at approximate slack length on cork. TA muscles were also pinned at slack length on cork prior to decellularization. Pinned samples were placed in tubes containing 50 nM latrunculin B (Cayman Chemical, Ann Arbor, MI) in high glucose Dulbecco's modified Eagle's medium (DMEM; Gibco, Carlsbad, CA) for 2 h at 37 °C with agitation. Samples were then placed in separate wells of a 6 well plate and washed with deionized (DI) water twice for 15 min at room temperature with agitation. The remainder of the steps occurred at room temperature with agitation. Muscles were then incubated in 0.6 M potassium chloride (Thermo Fisher Scientific, Waltham, MA) for 2 h, washed with DI water

twice for 15 min, and incubated in 1.0 M potassium iodide (Thermo Fisher Scientific, Waltham, MA) for 2 h. Samples were then left in DI water overnight. The following day the potassium chloride and potassium iodide incubations were repeated with two 15-minute DI washes after each incubation step. Samples were then treated for 2 h with DNase I (10U/ml; Thermo Fisher Scientific, Waltham, MA) in a buffer containing 130 μM $CaCl_2$, 5 mM MgCl, and 10 mM Tris-HCl with a pH of 7.50; after this treatment was complete, the samples were left on DI water overnight. The following day the DI water was replaced on the samples; mechanical testing and storage took place the next day after an additional replacement of DI water.

Collagenase digestion protocol

Collagenase digestion was performed similarly to a previous study [41]. In line with product manufacturer instructions, type II collagenase (Gibco, Carlsbad, CA) was added to 1 ml of Hank's Balanced Salt Solution with calcium, magnesium, and no phenol red (Gibco, Carlsbad, CA) and then vortexed to mix. Prior to collagenase treatment, collagenase stock solution was thawed on ice and diluted to 200U/mL in modified Rees-Simpson solution (109 mM sodium chloride, 25 mM sodium bicarbonate, 5 mM potassium chloride, 5 mM N,N'-bis[2-hydroxyethyl]-2-aminoe thanesulfonic acid buffer, 2 mM calcium chloride, 1 mM magnesium chloride, 0.4 mM glutamine, 0.3 mM glutamic acid) [41,66]. Following muscle isolation and/or mechanical testing EDL, soleus, and diaphragm muscles were pinned at L_o on cork. Gastrocnemius muscles were each cut in half longitudinally and were pinned at approximate slack length on cork. One half of gastrocnemius muscles were digested in collagenase while the other was stored without digestion. TA muscles were also pinned at slack length on cork prior to treatment. Pinned muscles were placed in a tube containing Rees-Simpson solution with 200U/mL collagenase and were incubated for 1 h at 37 °C with agitation. After incubation samples were placed in 6 well plates containing phosphate-buffered saline (PBS) for two 5-minute washes before mechanical testing or storage of samples.

Hydroxyproline assay

Following mechanical testing and storage EDL, soleus, and diaphragm muscles were assayed for collagen content and cross-linking using the hydroxyproline and collagen solubility protocols similar to other studies [21,67,68] and as described previously [20,23]. Muscles were removed from −80 °C storage and powdered on dry ice with mortar and pestle. Powdered tissue was massed and then suspended in PBS and stirred for 30 min at 4 °C. Samples were then centrifuged at 21,000g for 30 min at 4 °C and the supernatant was discarded. Sample pellets were resuspended in 0.5 M Acetic Acid containing 1 mg/ml pepsin and stirred overnight at 4 °C. The next day samples were centrifuged for 30 min at 21,000g at 4 °C before separating the supernatant (soluble fraction) and pellet (insoluble fraction). The soluble fraction was boiled off on a hot plate and then both fractions were separately combined with 6 N hydrochloric acid. A set of standard concentrations of hydroxyproline solution (0–1,000 μM *trans*-4-hydroxy-$_L$-proline; Fisher) were also combined with 6 N hydrochloric acid. All solutions were mixed and then boiled overnight at 105 °C. The following day 10 μl of each sample was aliquoted into new tubes for the remainder of the protocol. Isopropanol was added to each solution along with solution A (1 to 4 dilution of 7% chloramine-T (ThermoFisher) in water to acetate citrate buffer). Samples were mixed and left at room temperature for 10 min. Solution B (3 to 13 dilution of Erlich's reagent [1.5g of 4-(dimethylamino) benzaldehyde (ThermoFisher); 5 ml ethanol; 337 μl sulfuric acid] to isopropanol) was added to the solutions and each tube was mixed and placed in a 58 °C hot plate for 30 min. Samples were then put on ice and then centrifuged for 1 min at 5,000g at 4 °C. Final mixtures were aliquoted into a 96-well plate and absorbance was measured at 558 nm. Collagen content and cross-linking was back calculated using the standard curve and reported as μg collagen per mg powdered tissue mass.

Immunostaining and fluorescent imaging

TA muscle sections were fixed with 4% paraformaldehyde for 15 min and then washed three times for 5 min with PBS. 0.5% Triton was applied for 10 min to lyse the cells and then tissue was blocked with 0.1% bovine serum albumin (BSA) twice for 5 min each. A 5% BSA solution was left on the sections for 30 min before addition of primary antibodies diluted in 5% BSA. The primary antibody used was MF20c (1:500; DSHB Hybridoma Product MF 20). Following overnight incubation at 4 °C, sections were rinsed three times for 5 min with 0.1% BSA. Secondary antibodies diluted in 0.1% BSA were then applied to sections for 90 min in the dark. Sections were kept in the dark for the remainder of the protocol. The secondary antibody used was Donkey Anti-mouse 647 (1:500; Invitrogen A32787). At this step, other stains were applied including Wheat Germ Agglutinin (WGA) 488 (1:200; Invitrogen W7024) and Actistain 555 (1:250; Cytoskeleton PHDH7). After secondary antibody incubation, sections were rinsed three times for 5 min with 0.1% BSA. A Hoechst stain was then applied for 15 min to visualize nuclei (1:2000; Fisher H3570). Sections were then rinsed twice for 5 min with 0.1% BSA and then once more with PBS. Prolong

Gold (Fisher P36934) was applied to the sections and a coverslip was placed on top of the slide.

Stained sections were imaged by epifluorescence using an inverted Leica DMi8 microscope. A 20× objective was used to image each section by tile scan. Cy5, Rhodamine, FITC, and DAPI channels were used to image muscle sections. Tile scans were merged and analyzed for percent positive area. Each set of slides was imaged using the same settings, including intensity and exposure.

Sirius red staining and imaging

Picrosirius red staining and imaging was done similarly to previous studies [20,21,23,69,70]. Diaphragm, EDL, and soleus muscles were sectioned at −20 °C into 10 μm transverse slices. Sections were placed on glass slides and circled with a hydrophobic PAP pen before fixing in 4% paraformaldehyde for 10 min. Sections were then rinsed with distilled water three times for 5 min each and air dried for 15 min. Samples were stained in picrosirius red solution for 60 min and then washed twice in acidified water for 1 min each. Three 1-minute washes of 100% ethanol were applied to dehydrate the samples. Citrisolv was then applied for 3 min and Permount was left on the sections before a coverslip was placed on top.

Transverse sections were imaged with a 20X objective using brightfield illumination on a Leica DMi8 microscope and DFC9000GTC camera. Linearly polarized light imaging was utilized with a rotating polarizer in the beam path before and after the sample. Sirius Red Area and Collagen fiber density were quantified using a custom MatLab script (Mathworks, Natick, MA) and as previously described [21].

Statistical analysis

All statistical tests were performed in GraphPad Prism. T-tests were used to compare bodyweight, muscle length, and cross-sectional area between genotypes. One-way ANOVAs were run by treatment type (untreated, sham, collagenase; untreated, 1-hour collagenase, 2-hour collagenase) for validation and time course experiments. Post-hoc Tukey multiple comparisons tests were run to find specific differences between groups. Two-way ANOVAs were run by genotype (wildtype and D2.*mdx*) and by treatment (untreated versus collagenase digested or decellularized), strain (0–12.5%), or muscle (diaphragm and soleus). Post-hoc Sidak multiple comparisons tests were run to find specific differences between groups. Fit lines for stress–strain curves were fit using a second order polynomial regression. Unless otherwise stated, significance was set at $p < 0.05$. Data are reported in figures as mean ± SEM.

Funding

This work was supported by grants from the NIH National Institute of Arthritis and Musculoskeletal and Skin Diseases (NIAMS; R00AR067867 and R01AR079545) and the Hartwell Foundation.

CRediT authorship contribution statement

Ross P. Wohlgemuth: Conceptualization, Methodology, Software, Validation, Investigation, Resources, Visualization. **Ryan M. Feitzinger:** Validation, Investigation. **Kyle E. Henricson:** Investigation. **Daryl T. Dinh:** Validation, Investigation. **Sarah E. Brashear:** Investigation. **Lucas R. Smith:** Conceptualization, Methodology, Software, Resources, Visualization, Funding acquisition.

DATA AVAILABILITY

Data will be made available on request.

DECLARATION OF COMPETING INTEREST

The authors declare the following financial interests/personal relationships which may be considered as potential competing interests: Lucas Smith reports financial support was provided by National Institute of Arthritis and Musculoskeletal and Skin Diseases.

Acknowledgements

The work was supported by the labs of Drs. Keith Baar and Aldrin Gomes including access to equipment and attentive comments on the study. We would like to thank UC Davis graduate students Suraj Pathak, Danielle Steffen, Nathaniel Herrera, and additional members of the MyoMatrix Lab including CJ Mileti, Taryn Loomis, and Sathvik Sriram for insightful conversations and review of the data.

Appendix A. Supplementary data

Supplementary data to this article can be found online at https://doi.org/10.1016/j.mbplus.2023.100131.

Received 19 November 2022;
Accepted 9 March 2023;
Available online 13 March 2023

Keywords:
Fibrosis;
Skeletal Muscle Mechanics;
Muscular Dystrophy;

Decellularization; Collagenase

Abbreviations:
CD, collagenase digested; Coll-ase, collagenase; DCM, decellularized matrix; Decell, decellularized; DMD, Duchenne Muscular Dystrophy; DP, diaphragm; ECM, extracellular matrix; EDL, extensor digitorum longus; MyHC, myosin heavy chain; PCSA, physiological cross-sectional area; SOL, soleus; TA, tibialis anterior; WGA, wheat germ agglutinin; WT, wildtype

References

[1]. Gillies, A.R., Lieber, R.L., (2011). Structure and function of the skeletal muscle extracellular matrix. *Muscle Nerve*, **44**, 318–331. https://doi.org/10.1002/mus.22094.

[2]. Klingler, W., Jurkat-Rott, K., Lehmann-Horn, F., Schleip, R., (2012). The role of fibrosis in Duchenne muscular dystrophy. *Acta Myologica*, **31**, 184–195.

[3]. Deconinck, N., Dan, B., (2007). Pathophysiology of Duchenne Muscular Dystrophy: Current Hypotheses. *Pediatr. Neurol.*, **36**, 1–7. https://doi.org/10.1016/J.PEDIATRNEUROL.2006.09.016.

[4]. Hammers, D.W., Hart, C.C., Matheny, M.K., Wright, L.A., Armellini, M., Barton, E.R., et al., (2020). The D2.mdx mouse as a preclinical model of the skeletal muscle pathology associated with Duchenne muscular dystrophy. *Sci. Rep.*, **10**, 1–12. https://doi.org/10.1038/s41598-020-70987-y.

[5]. Ramaswamy, K.S., Palmer, M.L., van der Meulen, J.H., Renoux, A., Kostrominova, T.Y., Michele, D.E., et al., (2011). Lateral transmission of force is impaired in skeletal muscles of dystrophic mice and very old rats. *J. Physiol.*, **589**, 1195–1208. https://doi.org/10.1113/JPHYSIOL.2010.201921.

[6]. Moens P, Baatsen PHWW, Mari∼chal G. Increased susceptibility of EDL muscles from mdx mice to damage induced by contractions with stretch. vol. 14. 1993.

[7]. Petrof BJ. The molecular basis of activity-induced muscle injury in Duchenne muscular dystrophy. vol. 179. 1998.

[8]. Petrof, B.J., Shrager, J.B., Stedman, H.H., Kelly, A.M., Sweeney, H.L., (1993). Dystrophin protects the sarcolemma from stresses developed during muscle contraction. *PNAS*, **90**, 3710–3714. https://doi.org/10.1073/PNAS.90.8.3710.

[9]. Nigro, G., Comi, L.I., Limongelli, F.M., Giugliano, A.M., Politano, L., Petretta, V., et al., (1983). Prospective study of X-linked progressive muscular dystrophy in campania. *Muscle Nerve*, **6**, 253–262. https://doi.org/10.1002/mus.880060403.

[10]. Shimizu, J., Matsumura, K., Kawai, M., Kunimoto, M., (1991). Nakano I [X-ray CT of Duchenne muscular dystrophy skeletal muscles–chronological study for five years]. *Rinsho Shinkeigaku*, **31**, 953–959.

[11]. Joe AWB, Yi L, Natarajan A, le Grand F, So L, Wang J, et al. Muscle injury activates resident fibro/adipogenic progenitors that facilitate myogenesis 2010. 10.1038/ncb2015

[12]. Loomis, T., Hu, L.-Y., Wohlgemuth, R.P., Chellakudam, R.R., Muralidharan, P.D., Smith, L.R., (2022). Matrix stiffness and architecture drive fibro-adipogenic progenitors' activation into myofibroblasts. *Sci. Rep.*, **12**, 13582. https://doi.org/10.1038/s41598-022-17852-2.

[13]. Smith, L.R., Barton, E.R., (2018). Regulation of fibrosis in muscular dystrophy. *Matrix Biol.*, **68–69**, 602. https://doi.org/10.1016/J.MATBIO.2018.01.014.

[14]. Fadic, R., Mezzano, V., Alvarez, K., Cabrera, D., Holmgren, J., Brandan, E., (2006). Increase in decorin and biglycan in Duchenne muscular dystrophy: Role of fibroblasts as cell source of these proteoglycans in the disease. *J. Cell Mol. Med.*, **10**, 758–769. https://doi.org/10.1111/J.1582-4934.2006.TB00435.X.

[15]. Yan, W., Wang, P., Zhao, C.X., Tang, J., Xiao, X., Wang, D.W., (2009). Decorin gene delivery inhibits cardiac fibrosis in spontaneously hypertensive rats by modulation of transforming growth factor-beta/Smad and p38 mitogen-activated protein kinase signaling pathways. *Hum. Gene Ther.*, **20**, 1190–1200. https://doi.org/10.1089/HUM.2008.204/ASSET/IMAGES/LARGE/FIG-8.JPEG.

[16]. Bentzinger, C.F., Wang, Y.X., von Maltzahn, J., Soleimani, V.D., Yin, H., Rudnicki, M.A., (2013). Fibronectin regulates Wnt7a signaling and satellite cell expansion. *Cell Stem Cell*, **12**, 75–87. https://doi.org/10.1016/J.STEM.2012.09.015.

[17]. Lenselink, E.A., (2015). Role of fibronectin in normal wound healing. *Int. Wound J.*, **12**, 313–316. https://doi.org/10.1111/IWJ.12109.

[18]. Clark, R.A.F., (2001). Fibrin and Wound Healing. *Ann. N. Y. Acad. Sci.*, **936**, 355–367. https://doi.org/10.1111/J.1749-6632.2001.TB03522.X.

[19]. Fratzl, P., Misof, K., Zizak, I., Rapp, G., Amenitsch, H., Bernstorff, S., (1998). Fibrillar structure and mechanical properties of collagen. *J. Struct. Biol.*, **122**, 119–122. https://doi.org/10.1006/JSBI.1998.3966.

[20]. Brashear, S.E., Wohlgemuth, R.P., Gonzalez, G., Smith, L.R., (2021). Passive stiffness of fibrotic skeletal muscle in mdx mice relates to collagen architecture. *J. Physiol.*, **599**, 943–962. https://doi.org/10.1113/JP280656.

[21]. Smith, L.R., Barton, E.R., (2014). Collagen content does not alter the passive mechanical properties of fibrotic skeletal muscle in mdx mice. *Am. J. Physiol. Cell Physiol.*, **306** https://doi.org/10.1152/ajpcell.00383.2013.

[22]. Sahani, R., Hunter Wallace, C., Jones, B.K., Blemker, S. S., (2022). Diaphragm muscle fibrosis involves changes in collagen organization with mechanical implications in Duchenne muscular dystrophy. *J. Appl. Physiol.*, **132**, 653–672. https://doi.org/10.1152/JAPPLPHYSIOL.00248.2021/ASSET/IMAGES/LARGE/JAPPLPHYSIOL.00248.2021_F009.JPEG.

[23]. Brashear SE, Wohlgemuth RP, Hu L-YR, Jbeily EH, Christiansen BA, Smith LR. Collagen cross-links scale with passive stiffness in dystrophic mouse muscles, but are not altered with administration of lysyl oxidase inhibitor. PLoS One 2022;17:e0271776. 10.1101/2022.07.08.499292.

[24]. Chapman, M.A., Pichika, R., Lieber, R.L., (2015). Collagen crosslinking does not dictate stiffness in a transgenic mouse model of skeletal muscle fibrosis. *J. Biomech.*, **48**, 375–378. https://doi.org/10.1016/J.JBIOMECH.2014.12.005.

[25]. Smith, L.R., Hammers, D.W., Lee Sweeney, H., Barton, E.R., (2016). Increased collagen cross-linking is a signature of dystrophin-deficient muscle. *Muscle Nerve*, **54**, 71–78. https://doi.org/10.1002/mus.24998.

[26]. Smith, L.R., Pichika, R., Meza, R.C., Gillies, A.R., Baliki, M.N., Chambers, H.G., et al., (2021). Contribution of extracellular matrix components to the stiffness of skeletal muscle contractures in patients with cerebral palsy. *Connect. Tissue Res.*, **62**, 287–298. https://doi.org/10.1080/03008207.2019.1694011.

[27]. van der Slot-Verhoeven, A.J., van Dura, E.A., Attema, J., Blauw, B., DeGroot, J., Huizinga, T.W.J., et al., (2005). The type of collagen cross-link determines the reversibility of experimental skin fibrosis. *Biochim. Biophys. Acta Mol. basis Dis.*, **1740**, 60–67. https://doi.org/10.1016/J.BBADIS.2005.02.007.

[28]. Vater, C.A., Harris, E.D., Siegel, R.C., (1979). Native cross-links in collagen fibrils induce resistance to human synovial collagenase. *Biochem. J*, **181**, 639–645. https://doi.org/10.1042/BJ1810639.

[29]. Piersma, B., Bank, R.A., (2019). Collagen cross-linking mediated by lysyl hydroxylase 2: an enzymatic battlefield to combat fibrosis. *Essays Biochem.*, **63**, 377–387. https://doi.org/10.1042/EBC20180051.

[30]. Mázala, D.A.G., Novak, J.S., Hogarth, M.W., Nearing, M., Adusumalli, P., Tully, C.B., et al., (2020). TGF-β–driven muscle degeneration and failed regeneration underlie disease onset in a DMD mouse model. JCI. *Insight*, **5** https://doi.org/10.1172/JCI.INSIGHT.135703.

[31]. Swaggart, K.A., Demonbreun, A.R., Vo, A.H., Swanson, K.E., Kim, E.Y., Fahrenbach, J.P., et al., (2014). Annexin A6 modifies muscular dystrophy by mediating sarcolemmal repair. *PNAS*, **111**, 6004–6009. https://doi.org/10.1073/PNAS.1324242111/SUPPL_FILE/SM07.AVI.

[32]. Buckley, M.R., Sarver, J.J., Freedman, B.R., Soslowsky, L.J., (2013). The dynamics of collagen uncrimping and lateral contraction in tendon and the effect of ionic concentration. *J. Biomech.*, **46**, 2242–2249. https://doi.org/10.1016/j.jbiomech.2013.06.029.

[33]. Screen, H.R.C., Bader, D.L., Lee, D.A., Shelton, J.C., (2004). Local Strain Measurement within Tendon. *Strain*, **40**, 157–163.

[34]. Meyer, G., Lieber, R.L., (2018). Muscle fibers bear a larger fraction of passive muscle tension in frogs compared with mice. *J. Exp. Biol.*,, 221. https://doi.org/10.1242/jeb.182089.

[35]. Meyer, G.A., Lieber, R.L., (2011). Elucidation of extracellular matrix mechanics from muscle fibers and fiber bundles. *J. Biomech.*, **44**, 771–773. https://doi.org/10.1016/J.JBIOMECH.2010.10.044.

[36]. Prado, L.G., Makarenko, I., Andresen, C., Krüger, M., Opitz, C.A., Linke, W.A., (2005). Isoform diversity of giant proteins in relation to passive and active contractile properties of rabbit skeletal muscles. *J. Gen. Physiol.*, **126**, 461–480. https://doi.org/10.1085/JGP.200509364.

[37]. Gillies, A.R., Smith, L.R., Lieber, R.L., Varghese, S., (2011). Method for decellularizing skeletal muscle without detergents or proteolytic enzymes. *Tissue Eng. Part C Methods*, **17**, 383–389. https://doi.org/10.1089/TEN.TEC.2010.0438.

[38]. Ward, S.R., Winters, T.M., O'Connor, S.M., Lieber, R.L., (2020). Non-linear Scaling of Passive Mechanical Properties in Fibers, Bundles, Fascicles and Whole Rabbit Muscles. *Front. Physiol.*, **11**, 211. https://doi.org/10.3389/FPHYS.2020.00211/BIBTEX.

[39]. Meyer, G.A., Lieber, R.L., (2012). Skeletal muscle fibrosis develops in response to desmin deletion. *Am. J. Physiol. Cell Physiol.*, **302**, 1609–1620. https://doi.org/10.1152/AJPCELL.00441.2011.

[40]. Reyna, W.E., Pichika, R., Ludvig, D., Perreault, E.J., (2020). Efficiency of skeletal muscle decellularization methods and their effects on the extracellular matrix. *J. Biomech.*,, 110. https://doi.org/10.1016/J.JBIOMECH.2020.109961.

[41]. Rowe, J., Chen, Q., Domire, Z.J., McCullough, M.B., Sieck, G., Zhan, W.Z., et al., (2010). Effect of collagen digestion on the passive elastic properties of diaphragm muscle in rat. *Med. Eng. Phys.*, **32**, 90–94. https://doi.org/10.1016/J.MEDENGPHY.2009.11.002.

[42]. Stedman, H., Sweeney, H., Shrager, J., Maguire, H., Panettieri, R., Petrof, B., et al., (1991). The mdx mouse diaphragm reproduces the degenerative changes of Duchenne muscular dystrophy. *Nature*, **352**, 536–539.

[43]. Stevens, E.D., Faulkner, J.A., (2000). The capacity of mdx mouse diaphragm to do oscillatory work. *J. Physiol.*, **522**, 457–466. https://doi.org/10.1111/j.1469-7793.2000.t01-3-00457.x.

[44]. Saini, K., Cho, S., Dooling, L.J., Discher, D.E., (2020). Tension in fibrils suppresses their enzymatic degradation – A molecular mechanism for 'use it or lose it'. *Matrix Biol.*, **85–86**, 34–46. https://doi.org/10.1016/J.MATBIO.2019.06.001.

[45]. Flynn, B.P., Bhole, A.P., Saeidi, N., Liles, M., Dimarzio, C.A., Ruberti, J.W., (2010). Mechanical Strain Stabilizes Reconstituted Collagen Fibrils against Enzymatic Degradation by Mammalian Collagenase Matrix Metalloproteinase 8 (MMP-8). *PLoS One*, **5**, e12337.

[46]. Puttini, S., Lekka, M., Dorchies, O.M., Saugy, D., Incitti, T., Ruegg, U., et al., (2009). Gene-mediated Restoration of Normal Myofiber Elasticity in Dystrophic Muscles. *Mol. Ther.*, **17**, 19–25. https://doi.org/10.1038/mt.2008.239.

[47]. van Zwieten, R.W., Puttini, S., Lekka, M., Witz, G., Gicquel-Zouida, E., Richard, I., et al., (2014). Assessing dystrophies and other muscle diseases at the nanometer scale by atomic force microscopy. *Nanomedicine (Lond.)*, **9**, 393–406. https://doi.org/10.2217/NNM.12.215.

[48]. Canelón, S.P., Wallace, J.M., (2019). Substrate Strain Mitigates Effects of β-Aminopropionitrile-Induced Reduction in Enzymatic Crosslinking. *Calcif. Tissue Int.*, **105**, 660–669. https://doi.org/10.1007/s00223-019-00603-3.

[49]. Williamson PR, Kittler JM, Thanassit JW, Kagan HM. Reactivity of a functional carbonyl moiety in bovine aortic lysyl oxidase Evidence against pyridoxal 5'-phosphate. vol. 235. 1986

[50]. Wu, Y., Wu, Y., Yang, Y., Yu, J., Wu, J., Liao, Z., et al., (2022). Lysyl oxidase-like 2 inhibitor rescues D-galactose-induced skeletal muscle fibrosis. *Aging Cell*,, 00. https://doi.org/10.1111/acel.13659.

[51]. Flores, J.M., Nascimento, B., Punjani, N., Salter, C.A., Bernie, H.L., Taniguchi, H., et al., (2022). Predictors of Curvature Improvement in Men With Peyronie's Disease Treated With Intralesional Collagenase Clostridium Histolyticum. *J. Sexual Med.*,. https://doi.org/10.1016/J.JSXM.2022.08.001.

[52]. Gelbard, M., Walsh, R., Kaufman, J.J., (1980). Clostridial collagenase and peyronie disease. *Urology*, **15**, 536. https://doi.org/10.1016/0090-4295(80)90028-X.

[53]. Badalamente, M.A., Hurst, L.C., (2000). Enzyme injection as nonsurgical treatment of Dupuytren's disease. *J. Hand Surgery*, **25**, 629–636. https://doi.org/10.1053/JHSU.2000.6918.

[54]. Starkweather, K.D., Lattuga, S., Hurst, L.C., Badalamente, M.A., Guilak, F., Sampson, S.P., et al., (1996). Collagenase in the treatment of Dupuytren's disease: An in vitro study. *J. Hand Surgery*, **21**, 490–495. https://doi.org/10.1016/S0363-5023(96)80368-6.

[55]. Hurst, L.C., Badalamente, M.A., Hentz, V.R., Hotchkiss, R.N., Thomas, F., Kaplan, D., et al., (2009). Injectable Collagenase Clostridium Histolyticum for Dupuytren's Contracture. *N. Engl. J. Med.*, **361**, 968–979.

[56]. Howard, J.J., Huntley, J.S., Graham, H.K., Herzog, W.L., (2019). Intramuscular injection of collagenase clostridium histolyticum may decrease spastic muscle contracture for children with cerebral palsy. *Med. Hypotheses*, **122**, 126–128. https://doi.org/10.1016/J.MEHY.2018.11.002.

[57]. Harrison, S.A., Abdelmalek, M.F., Caldwell, S., Shiffman, M.L., Diehl, A.M., Ghalib, R., et al., (2018). Simtuzumab Is Ineffective for Patients With Bridging Fibrosis or Compensated Cirrhosis Caused by Nonalcoholic Steatohepatitis. *Gastroenterology*, **155**, 1140–1153. https://doi.org/10.1053/J.GASTRO.2018.07.006.

[58]. Muir, A.J., Levy, C., Janssen, H.L.A., Montano-Loza, A.J., Shiffman, M.L., Caldwell, S., et al., (2019). Simtuzumab for Primary Sclerosing Cholangitis: Phase 2 Study Results With Insights on the Natural History of the Disease. *Hepatology*,, 69. https://doi.org/10.1002/hep.30237/suppinfo.

[59]. Bond MD, van Wart HE. Purification and Separation of Individual Collagenases of Clostridium histolyticum Using Red Dye Ligand Chromatography1. vol. 23. 1984

[60]. van Putten M, Putker K, Overzier M, Adamzek WA, Pasteuning-Vuhman S, Plomp JJ, et al. Natural disease history of the D2-mdx mouse model for Duchenne muscular dystrophy n.d. 10.1096/fj.201802488R.

[61]. Barton, E.R., Morris, L., Kawana, M., Bish, L.T., Toursel, T., (2005). Systemic administration of L-arginine benefits mdx skeletal muscle function. *Muscle Nerve*, **32**, 751–760. https://doi.org/10.1002/MUS.20425.

[62]. Petrof BJ, Stedman HH, Shrager JB, Eby J, Lee Sweeney H, Kelly AM, et al. Adaptations in myosin heavy chain expression and contractile function in dystrophic mouse diaphragm. 1993.

[63]. Mendez, J., Keys, A., (1960). Density and composition of mammalian muscle. *Metabolism*,, 184–188.

[64]. Hakim, C.H., Grange, R.W., Duan, D., (2011). The passive mechanical properties of the extensor digitorum longus muscle are compromised in 2-to 20-mo-old mdx mice. *J. Appl. Physiol.*, **110**, 1656–1663. https://doi.org/10.1152/japplphysiol.01425.2010.

[65]. Ward, S.R., Tomiya, A., Regev, G.J., Thacker, B.E., Benzl, R.C., Kim, C.W., et al., (2009). Passive mechanical properties of the lumbar multifidus muscle support its role as a stabilizer. *J. Biomech.*, **42**, 1384–1389. https://doi.org/10.1016/J.JBIOMECH.2008.09.042.

[66]. van der Heijden, H.F.M., Zhan, W.Z., Prakash, Y.S., Dekhuijzen, P.N.R., Sieck, G.C., (1998). Salbutamol enhances isotonic contractile properties of rat diaphragm muscle. *J. Appl. Physiol.*, **85**, 525–529. https://doi.org/10.1152/JAPPL.1998.85.2.525.

[67]. Heydemann, A., Huber, J.M., Demonbreun, A., Hadhazy, M., McNally, E.M., (2005). Genetic background influences muscular dystrophy. *Neuromuscul. Disord.*, **15**, 601–609. https://doi.org/10.1016/J.NMD.2005.05.004.

[68]. Flesch, M., Schiffer, F., Zolk, O., Pinto, Y., Rosenkranz, S., Hirth-Dietrich, C., et al., (1997). Contractile Systolic and Diastolic Dysfunction in Renin-Induced Hypertensive Cardiomyopathy. *Hypertension*, **30**, 383–391. https://doi.org/10.1161/01.HYP.30.3.383/FORMAT/EPUB.

[69]. Acuña, M.J., Pessina, P., Olguin, H., Cabrera, D., Vio, C. P., Bader, M., et al., (2014). Restoration of muscle strength in dystrophic muscle by angiotensin-1-7 through inhibition of TGF-b signalling. *Hum. Mol. Genet.*, **23**, 1237–1249. https://doi.org/10.1093/hmg/ddt514.

[70]. Trensz F, Haroun S, Cloutier A, Richter MV, Grenier G. A muscle resident cell population promotes fibrosis in hindlimb skeletal muscles of mdx mice through the Wnt canonical pathway. Am J Physiol-Cell Physiol 2010;299: C939–47. 10.1152/ajpcell.00253.2010.-Previous